ELSEVIER

Polymer 42 (2001) 8207–8216

polymer

www.elsevier.nl/locate/polymer

Temperature dependence of the photoluminescence in poly(ethylene terephthalate) films

G. Teyssèdre[a,*], J. Menegotto[b], C. Laurent[a]

[a]*Laboratoire de Génie Electrique, Université Paul Sabatier, 118 route de Narbonne, 31062 Toulouse, France.*
[b]*Laboratoire de Physique des Polymères, Université Paul Sabatier, 118 route de Narbonne, 31062 Toulouse, France.*

Received 13 April 2000; received in revised form 3 April 2001; accepted 25 April 2001

Abstract

Temperature effects on the photoluminescence spectrum, phosphorescence lifetime and phosphorescence intensity of poly(ethylene terephthalate) have been investigated in the range −185 to +30°C. Both the fluorescence and phosphorescence emission spectra are composed of a monomeric-like component and a red-shifted emission attributed to the formation of ground state dimers. Monomeric emissions are enhanced at low temperature. The transient phosphorescence signals at excitation switch-on and switch-off are clearly not exponential, but could be suitably fitted to a stretched-exponential function. The temperature dependence of the related parameters is discussed. The kinetic analyses of temperature effects on steady-state phosphorescence indicated that phosphorescence quenching is controlled by oxygen diffusion. A correlation between the phosphorescence decay and the secondary relaxation of PET as probed by dielectric spectroscopy has been established.

Keywords: Poly(ethylene terephthalate); Photoluminescence; Phosphorescence lifetime

1. Introduction

Over the last 30 years, considerable interest has been devoted to the study of optical properties of Poly(ethylene terephthalate), and, as part of it, to the room temperature photoluminescence. Indeed, PET has major applications in fibre industry and packaging, and optical properties as a whole are known to be dependent on processing-induced structural features such as crystallinity ratio and molecular orientation and give information at a molecular scale. Molecular orientation induced upon drawing has been investigated using the fluorescence polarisation anisotropy of either physically incorporated dyes [1], or chain-intrinsic chromophores [2,3]. Besides, PET is widely used in electrical engineering for its insulation properties. For such applications, high electrical strength and resistance to long-term degradation are required. The analysis of the optical signature of insulating materials submitted to high electrical stress constitutes a way of investigating space charge mediated electrical degradation [4–6]. Such analyses are all the more suited that the nature of the emitting groups is identified. Photoluminescence therefore constitutes a prerequisite to such investigations.

Progress in the understanding of the fluorescence of PET has been accomplished with the evidence of a ground-state dimer emission related to the amorphous phase of the material [2,7,8]. This feature has been demonstrated recently on more theoretical grounds [9,10]. Phosphorescence of PET and its temperature dependence has been comparatively less investigated [7,9,11]. Besides, the scarce phosphorescence spectra, which are reported, differ from one work to another [9,12]. The aim of this paper is to propose a detailed analysis of the temperature dependence of photoluminescence in PET. The evolution of the emission spectrum and the phosphorescence lifetime as a function of temperature are specifically considered. Correlation has been established between the temperature dependence of the phosphorescence and the secondary relaxation of PET as probed by dielectric dynamic analysis.

2. Experimental

2.1. Material

Non-oriented PET films of 200 μm thickness, $M_w = 20,000\ g\ mol^{-1}$, from Rhône–Poulenc have been investigated. Though nominally amorphous, samples appeared slightly hazy. The differential scanning calorimetry (DSC)

* Corresponding author. Fax: +33-5-6155-6452.
E-mail address: teyssedr@lget.ups-tlse.fr (G. Teyssèdre).

0032-3861/01/$ - see front matter
PII: S0032-3861(01)00306-8

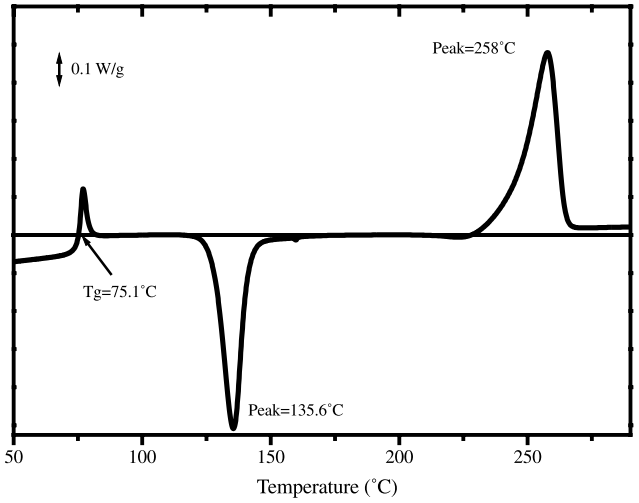

Fig. 1. DSC thermogram of PET obtained at a heating rate of 10°C min.

scan of the material is shown in Fig. 1. It was obtained with a DSC-2010-CE model from TA Instruments on a 16.9 mg sample and a heating rate of 10°C min^{-1}. The endothermic phenomenon characteristic of physical ageing effects peaks at 77°C. The glass transition defined at the intersection point of the DSC scan with the baseline extrapolated from the higher temperature signal is found at 75.1°C. The cold crystallisation peak is found at 135.6°C, and the melting peak at 258°C. The crystallinity has been estimated by two methods, first from the net heat flow integrated over the range 110–270°C, and second by integrating the cold crystallisation and melting peaks separately. The results are given in Table 1. Considering that the melting enthalpy for PET crystals is 119.8 J g^{-1} [13], crystallinity values of 12 and 8.5%, with the first and second methods, respectively, were deduced. Hence, the crystallinity of the materials can be estimated as ca. 10%.

2.2. Optical measurements

Photoluminescence measurements were realised using an home-made apparatus. A schematic representation of the optical arrangement is shown in Fig. 2. The experimental set-up is designed in such a way that low level light

Table 1
Parameters related to cold crystallisation and melting deduced from DSC. The peak area was deduced in respect to the baseline taken at the temperature limits given in the first column

Temperature range (°C)	Peak temperature (°C)	Transition enthalpy (J g^{-1})	Crystallinity (%)
110–270	–	14.40 (net)	12
110–190	135.6	−34.26 (crystallisation)	
200–280	258.0	44.38 (melting)	8.5

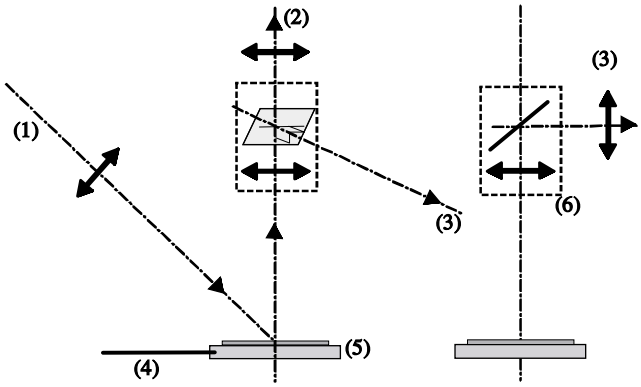

Fig. 2. Schematic diagram of the optical arrangement. (1) UV-excitation; (2) photon counting; (3) spectral analysis; (4) T-sensor; (5) sample and thermally regulated holder; (6) moving mirror holder.

emission from polymers may be measured in situ for various kinds of excitation, being either electrical field [4–6], cold plasma [14], UV or temperature [15]. The light tight chamber is organised around three optical axes equipped with windows and lenses made of quartz. The UV excitation for photoluminescence measurement is made on axis 1 using a 150W Xenon source coupled to a double-pass monochromator (Jobin–Yvon type H10). The available range of excitation wavelength is 220–800 nm. In the configuration used, the bandwidth of excitation is ≈ 2 nm.

On axis 2, integral light detection is made by means of a cooled (−20°C) photomultiplier (Hamamatsu R943-02) working in photon counting mode with Ortec counting electronics. A wide bandwidth (≈ 40 nm) filter can be inserted on the optical path for determining the phosphorescence lifetime. The spectral analysis of the emitted light is made on axis 3 using a grating monochromator (Jobin Yvon CP200) coupled to a liquid nitrogen cooled charge-coupled device -CCD- camera from Princeton. A mirror is moved on axis 2 for deflecting the light along axis 3 when spectra are recorded. The analysis range is 220–840 nm and the resolution is 4.5 nm in the configuration used. For both integral and wavelength resolved detection, the light is collected along a direction perpendicular to the plane of the sample film (axis 2).

The film sample is installed on a polished electrode and the specular reflection of the excitation beam is along an axis out of the solid angle of detection. The sample holder is thermally regulated by means of a heating resistor associated with a liquid nitrogen reservoir with continuous flow. The available temperature range is −185 to 180°C. All photoluminescence measurements were made in a Helium atmosphere at atmospheric pressure.

2.3. Dielectric spectroscopy

In order to establish correlations between the temperature dependence of photoluminescence and molecular motions related to the β-relaxation of PET, dielectric dynamic

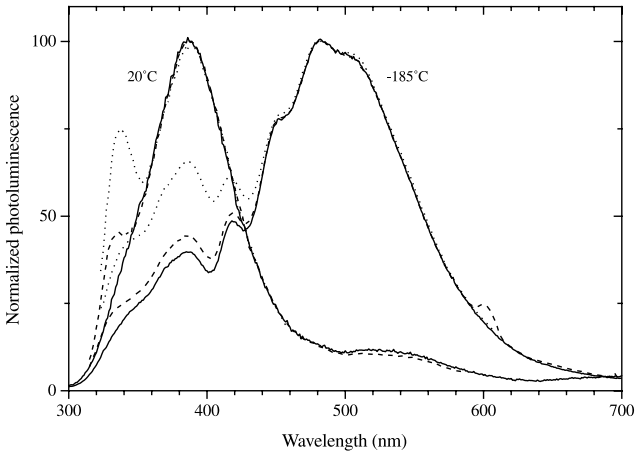

Fig. 3. Photoluminescence spectra obtained at 20 and −185°C, for different excitation wavelength: 280 nm = solid line; 300 nm = dashed line; 310 nm = dotted line. Spectra were normalised to the maximum emission.

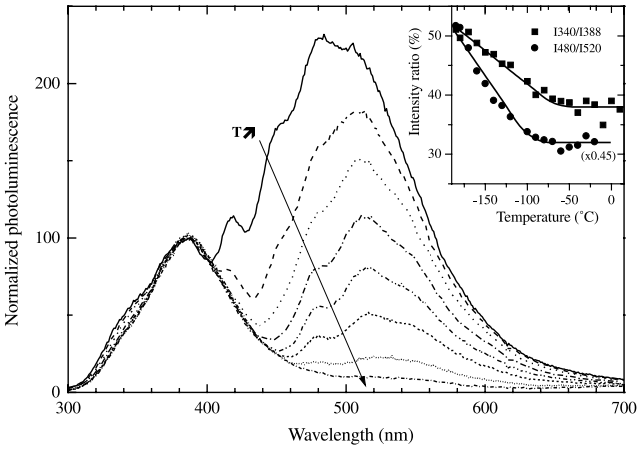

Fig. 4. Photoluminescence spectra obtained in 30°C step in the temperature range −180 to +30°C. Excitation wavelength = 280 nm. Spectra were normalised to the emission at 388 nm. The intensity ratio I340/I388 and I480/I520 are plotted in inset.

measurements were performed in the frequency range of 10^{-2}–10^{6} Hz with a Novocontrol BDS 4000 system, and in the temperature range of −150 to +20°C. More details on the set-up are given elsewhere [16].

3. Results and discussion

3.1. Photoluminescence spectrum

Fig. 3 compares the emission spectra obtained at different temperatures and excitation wavelengths. At room temperature, two bands are observed at 336 and 386 nm. The structured emission of fluorescence has already been extensively studied. The generally admitted interpretation is that the lower wavelength emission corresponds to the monomeric emission of PET. The longer wavelength, in the region 365–390 nm, has been interpreted as an excimeric emission [12,17,18] or a ground-state dimer [2,7,19,20]. Unlike excimers, which result from interaction of nearby excited states, and dissociate once relaxed to their ground state, ground-state dimers are stable states formed by interacting aromatic groups. It means that the excitation spectra of monomeric and excimeric emission are the same, whereas it is, in principle, different in case of ground state dimers [2]. In addition, excimer fluorescence of polymers is usually not polarised whereas dimer fluorescence can be polarised. The dimer emission is the most generally admitted interpretation specially, as regards this last criterion [2] even though it was occasionally contended [21,22]. Besides, the formation of ground state dimers requires that nearby aromatic rings belonging to different polymeric chains are close enough to produce interactions. Hemker et al. [23] observed an enhancement of this emission by uniaxial or biaxial orientation of the films, and proposed to use it as a probe of orientation changes in the material. Orientation is expected to increase interaction between nearby aromatic rings thereby favouring ground-state dimers formation. Moreover, it was shown that in the crystalline phase of PET, the interplanar distance of aromatic rings is too large so as to strongly interact [10]. The conclusion is that if ground-state dimers are formed, they necessarily concern the amorphous region of the material, which is fearly consistent with the relative strengthening of this band when the crystallinity of the material is lowered [18,24]. The dominance of the 386 nm emission in the investigated material (cf. Fig. 3) is consistent with the low crystallinity.

The photoluminescence spectrum exhibits no significant variation when changing the excitation wavelength in the range 220–280 nm, whatever the temperature is. Therefore, the corresponding spectra are not represented. For higher excitation wavelength, some evolution is observed as depicted in Fig. 3. The monomeric emission is relatively strengthened, which is again consistent with literature data: a sharp excitation peak at 310 nm has been reported for the monomeric emission whereas the excitation spectrum for the dimer emission is red-shifted to 325–340 nm [2,7,23]. Low temperature fluorescence spectra exhibit the structured dimer emission at 368 and 385 nm as already reported [3].

At low temperature, a structured phosphorescence emission is found with new bands at 420, 452, 482, 508, and 540 nm. These results are fearly consistent with the ones obtained by Takai et al. [12,25] in PET films. More recently, Lafemina and Arjavalingam [9] found extra bands at approximately 510 and 534 nm, in an unspecified sample form. However, in several works, only the lowest wavelength bands are seen: 424, 453, and 476 nm by Padhye and Tamhane [26] in films, and approximately the same results for PET in solution [17].

A closer insight into the behaviour of this material indicates that indeed two emission processes contribute to phosphorescence. Fig. 4 shows spectra obtained at 30°C intervals

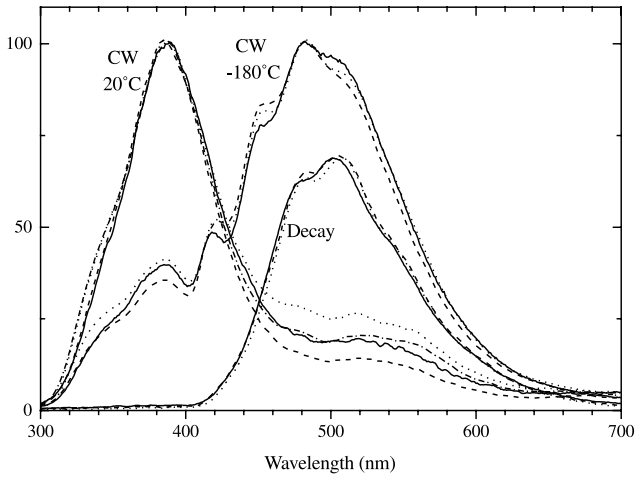

Fig. 5. CW photoluminescence spectra compared to the low temperature phosphorescence decay spectrum. Excitation wavelength = 280 nm. Data related to different samples are superimposed.

in the range −180 to +30°C with 280 nm as excitation wavelength. The short wavelength part of the phosphorescence spectrum quickly disappears as the temperature is raised whereas the longer wavelength part remains, and is even detectable at room temperature. As experiments were undertaken in a Helium atmosphere, the cell was previously pumped out down to about 5×10^{-3} Pa, and then helium was introduced as thermal exchange gas. A clear increase of the emission at around 500 nm was observed when comparing spectra obtained in air and in Helium, consistently with oxygen removal effects on phosphorescence yield. Temperature effects could also be detected on the fluorescence spectrum: the intensity of the band at 340 nm decreased relatively to the one at 385 nm. The temperature variations of the relative amplitudes of the fluorescence bands, I340/I388, and of the phosphorescence bands, I480/I520 are plotted in the inset of Fig. 4. A parallel effect is observed in the fluorescence and phosphorescence regions: These ratio decrease in the low temperature region, and seem approximately constant above −80°C. This behaviour provides a further indication that two kinds of species are being probed. Temperature effects coupled to emission variations upon excitation conditions (cf. Fig. 3) support the proposal that fluorescence at 340 nm and phosphorescence in the region 420–480 nm are both related to monomeric emission, whereas fluorescence at 385 nm and phosphorescence at around 500 nm would be both related to a different specie. An unresolved problem is the relative increase of the emission in the fluorescence region with respect to the phosphorescence region when the excitation wavelength is increased (cf. Fig. 3). It means that triplet states are populated by processes other than the direct intersystem crossing from the emitting singlet states.

In Fig. 5, we compare the continuous wave (CW) photoluminescence spectra obtained at room and liquid nitrogen temperature to the phosphorescence spectrum obtained after excitation was switched off. Not only the fluorescence emission, but also the low wavelength region of the phosphorescence spectrum decay instantaneously, in the time scale of the experiment ($t > 0.1$ s), whereas the longer wavelength part of the phosphorescence decays with a rate constant of the order of 1 s. In connection to these features, it is worth considering the conditions of excitation in relation to spectral features. As shown in Section 3.2, the phosphorescence build up follows the same kinetics as the decay. It means that under short pulse excitation, like with pulsed laser, short-lived species are preferentially excited, whereas under continuous excitation, longer-lived species can also be detected. These facts might explain the difference in phosphorescence spectra reported by different research groups.

The phosphorescence bands found below 500 nm have been interpreted as monomeric phosphorescence of $^3(\pi-\pi^*)$ states in view of the strong similitude with the model compound of PET, dimethyl terephthalate (DMT) emission [7,26], and considering computation results [9]. Takai et al. gave no assignment to the long wavelength components of phosphorescence. As a commercial material is characterised, one cannot exclude the possibility of residual impurities emission incorporated in PET chains. As example, this structured emission recalls the one obtained in copolymers of ethylene terephthalate and low content of 2.6 naphthalene dicarboxylate (PET-*co*-ND) [11]. The ND units differ from terephthalate ones through the replacement of the phenyl ring by naphthalene one. Even for low molar content of ND (2 mol%), the phosphorescence of PET is completely quenched with simultaneous sensitisation of ND phosphorescence with bands at 510, 550, and 600 nm [11]. Besides, ND moieties fluoresce at 390 nm. Though these features would be consistent with the results reported here, this possibility seems unlikely. First, if ND moieties are involved, one can admit that the apparent phosphorescence lifetime of PET, which is usually [7,11,26] of the order of 0.5–1 s, decrease, because of quenching effects by ND, so that the corresponding spectrum can no longer be detected in the decay spectrum. However, Cheung et al. [11] observed that the 390 nm fluorescence of the copolymers is delayed fluorescence resulting from triplet–triplet annihilation of ND moieties. Therefore, this band should decay with the same lifetime as the long-wavelength part of the phosphorescence spectrum, which is not the case in Fig. 5, consistently with fluorescence decay measurements [23]. Second, we have recently carried out photoluminescence measurements on a different source of PET, from Mitsubishi Chemicals. Fluorescence and phosphorescence exhibit qualitatively the same features, considering bands position, decay, and temperature effects. Hence, it seems that the results reported therein are characteristic of the very nature of PET. We have also checked the sample-to-sample reproducibility of the PL results using and the related results are reported in Fig. 5 for an excitation wavelength of 280 nm. The overall change in emission yield did not exceed 10%

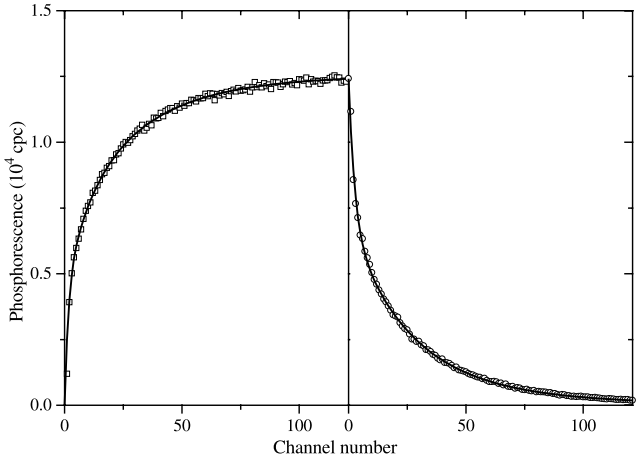

Fig. 6. Phosphorescence build-up and decay recorded using a counting dwell time of 50 ms. Lines are fits to the sum of three exponential functions. cpc stands for counts per channel. Excitation wavelength = 280 nm.

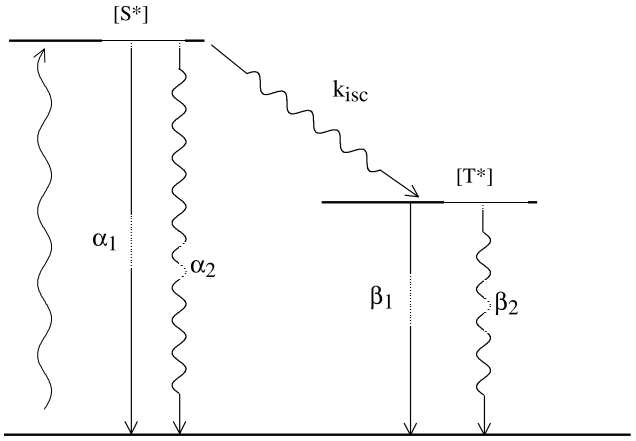

Fig. 7. Simplified energy diagram and rate constants for radiative (α_1) and non radiative (α_2) singlet excited state relaxation, inter-system crossing (k_{isc}), and radiative (β_1) and non radiative (β_2) triplet excited state relaxation.

from sample to sample, and part of it can be due to differences in sample positioning. At room temperature, the main variations concern the phosphorescence region. This is easily explained by the fact that emission in this region depended on the time the sample rested in vacuum or Helium atmosphere, i.e. the residual oxygen concentration within the film. The overall structures described above are detected for all the samples.

Hence, ND moieties are apparently not involved in the long wavelength bands of fluorescence and phosphorescence. Though chemical analyses would be necessary to definitively discard the possibility of impurities, they are not available at present. One of the reasons is that the films are too thick for being characterised by FTIR. The alternative interpretation is the one proposed by Lafemina et al. [9] who deduced from molecular dynamics simulation that the 540 nm emission might correspond to the phosphorescence of the ground-state dimer identified in fluorescence. So, the long wavelength structure of phosphorescence, i.e. essentially the phosphorescence decay spectrum of Fig. 5, possibly arises from these species. It would be consistent with the relatively strong emission found in this work at 385 nm in comparison to other works. However, a question mark remains on the nature of the actual structural features, which lead to a strong ground state dimer phosphorescence in some materials and to a weak emission in others.

3.2. Phosphorescence decay kinetics

Quantitative measurements of the temperature dependence of the CW phosphorescence and of its decay kinetics has been achieved by integral light detection through a large band-pass (40 nm) optical filter centred at 500 nm. The excitation wavelength was set at 280 nm for the whole measurements.

Fig. 6 shows a typical phosphorescence build-up and decay curve obtained at −185°C using a counting dwelling time of 50 ms. We can observe that within the excitation time of 6 s, the CW level of phosphorescence is not completely reached. Besides, the kinetics of build-up and decay appear the same at first sight. This behaviour has been reported for long [27,28]. It can be explained considering the simplified energy diagram of Fig. 7. Under continuous illumination, the triplet excited states formation is governed by first-order kinetics, according to

$$\frac{dS^*}{dT} = \epsilon_s i_s - \alpha' S^*, \qquad \alpha' = \alpha_1 + \alpha_2 + k_{isc}, \tag{1}$$

$$\frac{dT^*}{dT} = k_{isc} S^* - \beta T^*, \qquad \beta = \beta_1 + \beta_2,$$

where ϵ_s is the absorption coefficient for the light intensity i_s, α and β are the rate constant for singlet and triplet excited states relaxation, respectively, the indexes 1 and 2 refer to radiative and non-radiative processes, respectively, and k_{isc} is the rate constant of inter-system crossing. If the sample is irradiated at $t = 0$, the density of triplet excited states deduced from Eq. (1) is given by

$$T^* = \frac{k_{isc}}{\alpha'\beta}\epsilon_s i_s\left[1 + \frac{\beta}{\alpha' - \beta}e^{-\alpha' t} - \frac{\alpha'}{\alpha' - \beta}e^{-\beta t}\right] \tag{2a}$$

and if the light is cut-off at $t = 0$ once the steady-state emission is reached, one gets

$$T^* = \frac{k_{isc}}{\alpha' - \beta}\epsilon_s i_s\left[\frac{1}{\beta}e^{-\beta t} - \frac{1}{\alpha'}e^{-\alpha' t}\right] \tag{2b}$$

The lifetime of singlet excited states is much shorter than the one of triplet states, i.e. $\alpha \gg \beta$. As the phosphorescence emission is of the form $I \propto \beta_1 T^*$, the following transient

Table 2
Fit parameters of phosphorescence build-up and decay obtained at −185°C using counting dwell times of 50 and 10 ms. cpc stands for counts per channel. The % error bars are given in brackets. (*): Constrain on ΣI_i set to the value obtained at the end of the CW irradiation

Parameter	DT = 50 ms excitation	DT = 50 ms decay	DT = 10 ms excitation	DT = 10 ms decay
I_{cw} (cpc)	12,540 (0.5%)	12,410*	2498 (0.2%)	2490*
I_1 (cpc)	4305 (23%)	5380 (2%)	813 (10%)	899 (5%)
I_2 (cpc)	2997 (30%)	5445 (2%)	696 (10%)	750 (3%)
I_3 (cpc)	5236 (23%)	1585 (8%)	989 (8%)	842 (2%)
τ_1 (ms)	77 (30%)	126 (4%)	1 (20%)	41 (7%)
τ_2 (ms)	515 (42%)	1160 (2%)	440 (11%)	640 (4%)
τ_3 (ms)	1620 (17%)	2600 (2%)	1650 (6%)	1880 (1%)

signals are predicted:

$$I_b \approx I_{cw}[1 - e^{-\beta t}] \qquad \text{with } I_{cw} \propto \frac{k_{isc}}{\alpha'}\frac{\beta_1}{\beta}\epsilon_s i_s \qquad \text{and :}$$

$$I_d \approx I_{cw} e^{-\beta t} \tag{3}$$

for the phosphorescence build-up (I_b) and decay (I_d), respectively. I_{cw} is the continuous wave emission. Eq. (3) shows that the both transients should be described by an exponential function with the same time constants.

The symmetric behaviour predicted by Eq. (3) is verified in Fig. 6. However, the phosphorescence build-up and decay could not be fitted to a single exponential law. A sum of at least three exponential functions was necessary to fit suitably these measurements:

$$I_b = I_{cw} - \sum_i I_i e^{-t/\tau i}, \qquad I_d = \sum_i I_i e^{-t/\tau_i} \tag{4}$$

with the constrains $I_{cw} = \sum I_i$ for the build-up, and $\sum I_i = I'$ for the decay, where I' is the signal at the end of the excitation period.

The parameters obtained by non-linear fitting to Eq. (4) (cf. Table 2) can suitably describe the whole information of Fig. 6. The point is that the set of parameters so deduced is on one hand accompanied with a relatively large incertitude interval, and on the other that one does not really find the symmetric behaviour in the kinetics, which would be expected from Eq. (3). Besides, the consistency with results obtained using counting dwelling time of 10 and 50 ms is not straightforward. These features mean that the parameterisation was overdimensioned due to an inappropriate model. Would the fit be adequate, the question remains on the physical meaning of three or more contributions with lifetimes of the order of seconds. Indeed, CW and decay spectra presented in Fig. 5 show that probably only two kinds of specie having significantly different lifetimes contribute to the emission.

The alternative way we used for fitting these data was to consider a stretched exponential as decay law:

$$I_b = I_{cw} - I_s e^{-(t/\tau)^\gamma}, \qquad I_d = I_s e^{-(t/\tau)^\gamma} \tag{5}$$

for the phosphorescence build-up and decay, respectively. I_s is the long-lived contribution to the phosphorescence decay, τ is the characteristic lifetime, and γ is the stretching factor ($0 < \gamma \leq 1$). This form of decay suitably fitted the response over the time range 0.1–10 s. However, it could not account for the fast decay at $t < 0.1$ s as shown in Fig. 8. This behaviour confirms the trend observed in the spectra, namely that a short-lived component, with lifetime of the order of 10–20 ms and spectral features below 500 nm, is superimposed to a relatively long-lived one, with emission peaking at about 500 nm. The kinetic analysis presented here is related to the latter. The parameters listed in Table 3 show the consistency of the results considering build-up and decay, and using different counting dwelling times. About 75–80% of the CW emission is accounted for by this component.

It has been shown for long that exponential relaxation is the exception rather than the rule, specially in solids. The stretched exponential, otherwise referred to as Kohlrausch–Williams–Watts function [29,30], reflects disorder in its most general sense, so long as a wide variety of condensed materials, among which defectuous crystals, mixed crystals and glasses, may display such relaxation function. Insofar as photoluminescence decay is concerned, the deviation from monoexponential behaviour results from the existence of parallel deactivation pathways of distributed characteristics. A distribution in the conformational arrangement of emitting

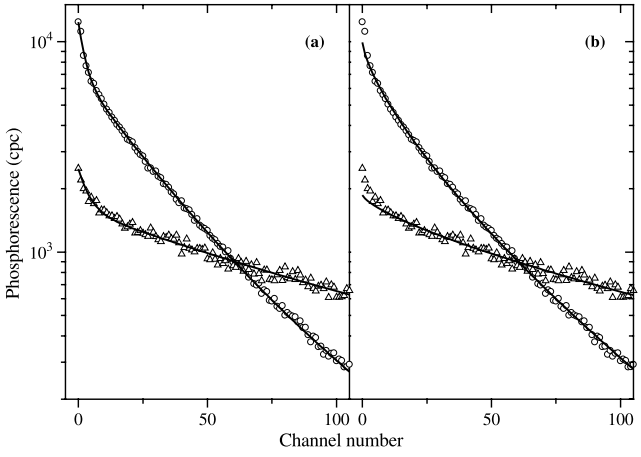

Fig. 8. Phosphorescence decay at −185°C using counting dwell time of 50 ms (circles) and 10 ms (triangles) fitted to the sum of three exponential functions (a) and stretched exponential (b).

Table 3
Fit parameters of phosphorescence build-up and decay obtained at −185°C using counting dwell times of 50 and 10 ms. cpc stands for counts per channel. The error bars are given in brackets. (*): set to I_s for the decay

Parameter	DT = 50 ms excitation	DT = 50 ms decay	DT = 10 ms excitation	DT = 10 ms decay
I_{cw} (cpc)	12,598 (0.6%)	–	2500 (0.2%)	–
I_s (cpc)	9915*	9915 (0.8%)	1865*	1865 (2%)
τ (ms)	876 (3%)	900 (1%)	866 (2%)	927 (2%)
β	0.715 (0.8%)	0.722 (0.6%)	0.720 (0.8%)	0.725 (2%)

species and of their interaction with surroundings groups, being either of the same nature or adventitious species, are possible sources of distribution. Even the fluorescence of PET exhibits distributed lifetimes [23]. Since in the present case phosphorescence is presumably related to ground state dimers, the relative orientation of nearby chromophores is a likely source of distribution.

Fig. 9 shows the temperature dependence of the shape parameters for the stretched exponential function obtained when analysing the decay signal. The signal intensity I_{cw} and I_s decrease in a parallel way, and describe a transition region between −100 and −50°C. The decay of fluorescence is superimposed on the same figure. It was monitored at 360 nm, in order to get rid of the variations of the 340 nm component on the one hand, and of a possible contribution of the phosphorescence tail spectrum on the other hand. The temperature variation is qualitatively similar to phosphorescence, but the amount of decay is much smaller. It means that mechanisms specific to triplet states are responsible for phosphorescence decay. The behaviour of the integral signal is discussed in Section 3.3 using more refined acquisition steps.

As the lifetime of triplet-excited states is relatively long, they have a great probability to transfer their energy to the surrounding, and the emission is henceforth quenched. Molecular oxygen is known as a very efficient quencher. Lowering the temperature freezes molecular groups in a certain configuration and reduces the probability of interaction between chromophores and molecular oxygen. Hence, the temperature dependence of phosphorescence has some relationships to relaxation processes involving local molecular motion as the diffusion of molecular oxygen as an example [31]. The phosphorescence features in a series of polymeric materials of variable nature has been successfully explained in terms of the accessibility of oxygen to chromophores in relation to secondary relaxations of the materials [32]. The transition region observed here between −50 and −100°C, is most probably related to the β-relaxation of PET, as discussed in Section 3.3.

The temperature dependence of the phosphorescence yield has been considered so far in a wide variety of polymers [32,33], but the decay kinetics is surprisingly limited to rather specific materials such as poly(*N*-vinylcarbazole) [34] or dies-doped polymers [35]. Nevertheless, for an exponential decay, a direct relationship is predicted from Eq. (3): neglecting to a first approximation temperature effects on fluorescence features and inter-system crossing [32], the steady state emission would be of the form: $I_{cw} \propto \beta_1 \tau$. The measured apparent lifetime $\tau = (\beta_1 + \beta_2)^{-1}$, which is lower than the intrinsic, essentially temperature-independent [35,36] radiative lifetime, β_1^{-1}, should depend on temperature essentially through the non-radiative term, β_2, in a way similar to the intensity. However, in the present situation, such analysis is not straightforward because the decay is not exponential, and the origin of the nonexponentiallity is not known. Fig. 9 shows that, in the low temperature region, i.e. up to about −80°C, the lifetime is practically constant at about 1 s whereas the stretching factor increases continuously from about 0.75 up to 0.90. Both parameters quickly decrease above −50°C. In order to give a picture of the decay kinetics, we have plotted in Fig. 10(a) the decay functions obtained at temperature intervals of 30°C. One can visually conclude that the

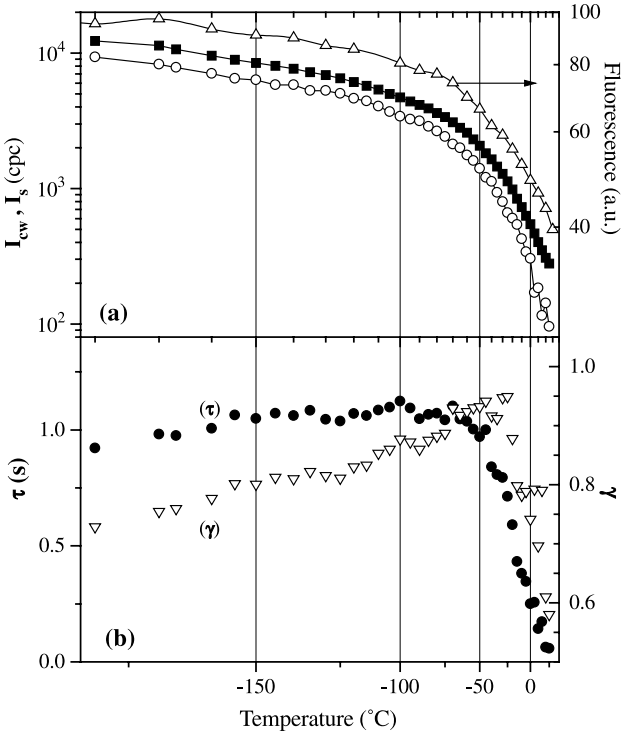

Fig. 9. Temperature dependence of (a) CW phosphorescence (squares), fit parameter I_s for the initial intensity of the decay (circles), and fluorescence monitored at 360 nm (triangles); (b) relaxation time and stretching factor deduced from fit. X-scale is a reciprocal temperature axis.

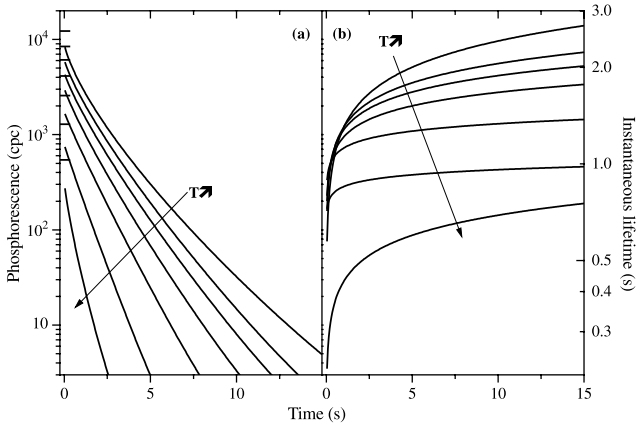

Fig. 10. (a) Decay functions in 30°C intervals from −180 to 0°C deduced from stretched-exponential fitting. (b) Instantaneous lifetime versus time deduced from (a).

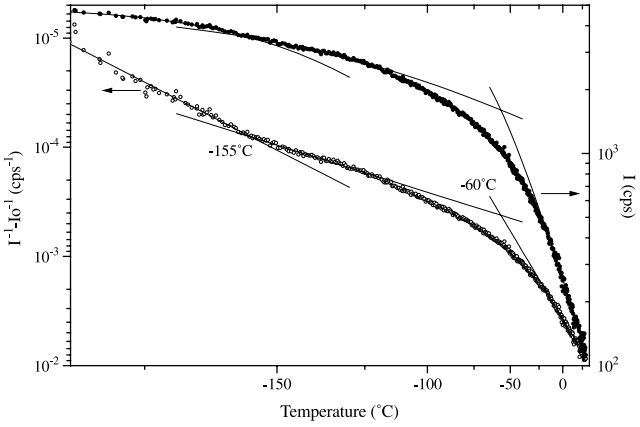

Fig. 11. Phosphorescence versus temperature in an Arrhenius diagram. cps stands for counts per second. The activation energies were deduced from the plot of $I^{-1} - I_0^{-1}$ vs. T^{-1}. Fit lines were reported on the I vs. T^{-1} plot.

decay is faster as the temperature is increased. From the stretched exponential function, one can determine an 'instantaneous' lifetime [37], defined as: $\tau_{\text{inst}}(t) = I(t)/|\mathrm{d}I(t)/\mathrm{d}t|$:

$$\tau_{\text{inst}}(t) = \gamma^{-1}\tau^{\gamma}t^{1-\gamma} \tag{6}$$

The variations of τ_{inst} versus time are plotted in Fig. 10(b). The combined variation of γ and τ lead to a significant decrease of the instantaneous lifetime when the temperature is increased. However, this decrease is smaller than one would expect from the temperature dependence of the CW emission and considering single exponential decay.

The increase of the stretching factor as the temperature is increased, i.e. the convergence to exponentiallity, can be explained by the progressive removal of the statistical distribution of deactivation pathways. The probability of interaction with oxygen possibly becomes more homogeneous as the temperature is reached. Either chromophores have the ability to explore, within their lifetime, all the possible configurations available, or, alternatively, within their lifetime, their environment has evolved so that they essentially behave all in the same way.

Ground state dimers possibly introduce specific photophysical properties. As discussed previously, their formation is conditioned by the possibility of interaction between nearby aromatic rings. Spectral analyses indicated that the monomeric emission disappears above ≈ -100°C. A possible reason is that the unfreezing of molecular motions favours interaction of nearby chromophores and increases the probability of formation of associated dimers. The monomeric emission would be quenched accordingly. Besides, a new quenching mechanism for triplet excited states of dimers can be envisaged if the mean interaction time between aromatic rings becomes of the same order as, or lower than, the radiative lifetime. Quenching would then correspond to the physical disappearance of the specie.

3.3. Relation with the β-relaxation of the material

The temperature dependence of the CW phosphorescence has been analysed in order to derive the activation energy in different temperature intervals. With the hypothesis that the phosphorescence deactivation rate can be divided into a temperature-independent term, say β_1, and a temperature-dependent term, β_2, according to an Arrhenius law, the phosphorescence intensity should depend on temperature according to [32,33]:

$$I^{-1} - I_0^{-1} = C\exp(-E_a/kT) \tag{7}$$

where I_0 is the low temperature limit of the intensity, and E_a is the activation energy. Fig. 11 shows the results of such an analysis obtained by approximating I_0 to the intensity for the lowest temperature achievable (−188°C). The measurements were done at a linear heating rate of 5°C min^{-1}, using a dwelling time of 1 s for photon counting. Three temperature intervals can be defined, and the corresponding activation energies are listed in Table 4. The intercept of the fit lines allows to define two transition temperatures at about −155 and −60°C. The decrease of the activation energy at −155°C probably reflects the changes in spectral features observed for the lowest temperatures. E_a for the short wavelength part of the phosphorescence spectrum is higher than the one for the longer wavelength part. The higher temperature transition does actually correspond to the β-relaxation of PET. The activation energy changes in a great extent across the relaxation. The values of E_a are in good agreement with

Table 4
Activation energies of CW phosphorescence decay calculated in the temperature range indicated in the first column

Temperature range (°C)	E_a (eV)
−185 to −155	0.060
−155 to −120	0.036
−20 to +30	0.195

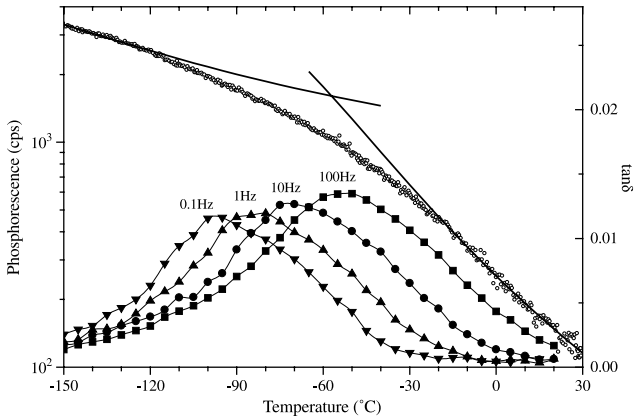

Fig. 12. Correlation between phosphorescence intensity and loss factor obtained in dielectric measurements at different frequencies. Lines are fits reported from Fig. 11.

those reported by Somersall et al. [32] for various polymers, on both sides of the relaxation. Besides, Light and Semour [38] established a clear relationship between the β-relaxation and oxygen diffusion and permeability in a series of polyesters including PET. The activation energies they deduced for the permeability of O_2 in PET were 0.056 and 0.30 eV, below and above the transition temperature $T_0 = -63$°C, respectively. The consistency of these values with the ones obtained in phosphorescence measurements constitutes a further strong indication that oxygen is responsible for the phosphorescence quenching.

Though the correlation between the gas transport properties and the sub-T_g molecular motions was established by considering the oxygen permeability and diffusivity versus strength of the mechanical relaxation for various polyesters [38], kinetics effects were not considered. The study of relaxation mechanisms from the standpoint of phosphorescence quantum yield and lifetime inevitably leads to the problem of the equivalent frequency since the observed temperature for a relaxation depends on the frequency used to probe it. With the hypotheses that: (i) the quantum yield attenuation when temperature is increased is due to quenching by adventitious species, e.g. oxygen, and (ii) polymer relaxations (specially local processes) produce an increase of the mobility of oxygen, or of any other quenching specie within the polymer, it can be inferred that the temperature at which a significant decrease of phosphorescence emission is observed is comparable to the isochronal secondary relaxation peak T_m probed at a frequency ω corresponding to the reciprocal of the lifetime. In other words, if phosphorescence is quenched by a process somehow linked to the relaxation, this process must happen within a time corresponding to the lifetime. In order for a quenching effect to be efficient, and so detectable, it must occur with a time constant shorter than the natural lifetime of the triplet states. The onset of such quenching effect is detected when the rate constants of triplet relaxation are such that $\beta_2 \cong \beta_1$. Therefore, the equivalent frequency of the phosphorescence dynamics measurement is $\omega_{eq} \cong \beta_1$. If species have a long phosphorescence lifetime, the appropriate frequency for dynamic measurements is accordingly lower. For the measurements made in this work, the equivalent frequency would be in the range 1–10 Hz.

Fig. 12 shows the temperature dependence of the dielectric loss factor for frequencies in the range 0.1–100 Hz. Measurements were made in isotherm conditions, in steps of 5°C, and then converted as isochrone curves. The mean activation energy for the dielectric β-relaxation has been estimated to 0.64 eV from data in the range 10^{-2}–10^{6} Hz. The mode is particularly broad as it is extending over more than 100°C. Several works undertaken with different techniques showed that it is constituted of two components, a lower temperature one ascribed to the motions of carbonyl groups, and an upper one corresponding to phenyl ring motions [16,39–41], which can be distinguished only at low frequency ($\approx 10^{-3}$ Hz) [16]. The broadness of the relaxation is reflected on the slow change of phosphorescence decay regime. Though it is difficult to define at which particular equivalent frequency phosphorescence decay correlates, due to the large transition range, an evident agreement is obtained between the two techniques. The activation energy of the dielectric relaxation and the one deduced from phosphorescence measurements are different and there is no reason that it be not so. In the low temperature side, phosphorescence decay in time is controlled by processes that are faster than sub-group motions, and the phosphorescence rate constant has a lower limit, which is the natural rate constant, β_1. In the high temperature side, local molecular motion is not the rate-limiting factor to oxygen transport, and so neither it is for phosphorescence quenching. So, correlation with dynamic experiments is expected for frequencies of the order of the natural rate constant of phosphorescence. Further validation of the approach would be obtained by considering polymers sensitivated with various dies having phosphorescence lifetime varying in a wide range.

4. Concluding remarks

Our objectives in this paper were to analyse the photophysical properties of poly(ethylene terephthalate). The information obtained in photoluminescence is of great importance for understanding emission of the material obtained by other methods, for example under excitation by an electric field. Indeed, we have shown that the electroluminescence spectrum of another polyester, poly(ethylene naphthalate), exhibits some components that are present in the photoluminescence spectrum, and some others that are not [5], which might constitute a signature of the field-induced degradation of the material. Besides, the electroluminescence spectrum of insulating polymers is usually dominated by phosphorescence, even at room temperature.

Further understanding of these features can be gained by considering the case of PET. However, one needs a thorough basic characterisation of its photoluminescence features.

The spectral analyses undertaken in this work have shown that at least two kinds of emitting specie coexist in PET. The interpretation of the different emissions has been made considering literature data on crystallinity and mechanical orientation effects on the photoluminescence of PET, complemented by the investigation of temperature effects on emission spectrum shape, emission intensity, and transient phosphorescence measurements.

A relatively weak monomeric-like fluorescence has been detected at 335 nm. The corresponding phosphorescence emission is structured with several bands in the region 420–480 nm, consistently with literature data. Stronger emissions were found at 385 nm in fluorescence, and in the range 480–540 nm in phosphorescence. The latter have been related to ground state dimers. Spectra taken at different temperatures showed that the relative contribution of both fluorescence and phosphorescence related to monomeric emissions decreased as the temperature was increased.

Transient phosphorescence has been analysed considering build-up and decay signals. Phosphorescence related to the monomeric emission has a much shorter lifetime of the order of 10–20 ms than the one related to ground state dimers. The transient signals related to the latter have been analysed using a stretched exponential function and the temperature dependence of the related parameters has been determined. The mean lifetime was constant ($\approx$1 s) at up to about -70°C, whereas the stretching factor continuously raised as the temperature was increased. Changes in the phosphorescence decay kinetics and in the phosphorescence intensity have been correlated to local motions related to the secondary relaxation of PET. The activation energies for the temperature dependence of the steady state phosphorescence, determined at the both sides of the β-relaxation, are consistent with the ones describing oxygen diffusion in the material, thereby confirming that molecular oxygen is the major factor controlling phosphorescence quenching.

References

[1] McGraw GE. J Polym Sci A2 1970;8:1323–36.
[2] Hennecke M, Fuhrman J. Makromol Chem: Macromol Symp 1986;5:181–6.
[3] Hennecke M, Kud A, Kurz K, Fuhrman J. Colloid Polym Sci 1987;265:674–80.
[4] Teyssedre G, Mary D, Laurent C, Mayoux C. In: Fothergill JC, Dissado LA, editors. Space charge in solid dielectrics. Leicester: Dielectrics Society Ed, 1998. p. 285–302 (Chapter 26).
[5] Teyssedre G, Mary D, Augé JL, Laurent C. J Phys D 1999;32:2296–305.
[6] Mary D, Albertini M, Laurent C. J Phys D 1997;30:171–84.
[7] Allen NS, McKellar JF. Makromol Chem 1978;179:523–6.
[8] Sonnenschein MF, Roland CM. Polymer 1990;31:2023–6.
[9] LaFemina JP, Arjavalingam G. J Phys Chem 1991;95:984–8.
[10] LaFemina JP, Carter DR, Bass MB. J Phys Chem 1992;96:2767–72.
[11] Cheung PSR, Roberts CW, Wagener KB. J Appl Polym Sci 1979;24:1809–30.
[12] Takai Y, Mizutani T, Ieda M. Jpn J Appl Phys 1978;17:651–8.
[13] Wunderlich B. Macromolecular physics, 1. New York: Academic Press, 1973. p. 389.
[14] Massines F, Tiemblo P, Teyssèdre G, Laurent C. J Appl Phys 1997;81:937–43.
[15] Tiemblo P, Gomez-Elvira JM, Teyssedre G, Massines F, Laurent C. Polym Degr Stab 1999;65:113–21.
[16] Menegotto J, Demont P, Bernes A, Lacabanne C. J Polym Sci B 1999;37:3494–503.
[17] Renuyan Q, Fenglian B, Shangxian C. Kexue Tongbao 1982;27:725–9.
[18] Cao T, Magonov SN, Qian R. Polym Commun 1988;29:43–4.
[19] Clauss B, Salem DR. Polymer 1992;33:3193–202.
[20] Hashimoto H, Hasegawa M, Horie K, Yamashita T, Ushiki H, Mita I. J Polym Sci: Phys Ed 1993;31:1187–96.
[21] Itagaki H, Inagaki Y, Kobayashi N. Polymer 1996;37:3553–8.
[22] Ouchi I, Miyamura R, Sakaguchi M, Hosaka S, Litagawa M. Polym Adv Technol 1999;10:195–8.
[23] Hemker DJ, Frank CW, Thomas JW. Polymer 1988;29:437–47.
[24] Itagaki H. J Lumin 1997;72–74:435–6.
[25] Takai Y, Mori K, Mizutani T, Ieda M. J Polym Sci: Phys Ed 1978;16:1861–8.
[26] Padhye MR, Tamhane PS. Angew Makromol Chem 1978;69:33–45.
[27] Randall JT. Trans Faraday Soc 1939;35:2–14.
[28] deGroot W. Trans Faraday Soc 1939;35:85–7.
[29] Kohlrausch R. Ann Phys (Leipzig) 1847;12:393.
[30] Williams G, Watts DC. Trans Faraday Soc 1970;66:80–5.
[31] Nishijima Y. J Polym Sci C 1970;31:353–73.
[32] Somersall AC, Dan E, Guillet JE. Macromolecules 1974;7:233–44.
[33] Rutherford H, Soutar I. J Polym Sci: Phys Ed 1977;15:2213–25.
[34] Burkhart RD, Aviles RG. J Phys Chem 1979;83:1897–901.
[35] Winnick MA, Pekcan O, Croucher MD. Can J Chem 1985;63:129–33.
[36] Jones PF, Siegel S. J Chem Phys 1969;50:1134–40.
[37] Dulieu B, Wery J, Lefrant S, Bullot J. Phys Rev B 1998;57:9118–27.
[38] Light RR, Seymour RW. Polym Engng Sci 1982;22:857–64.
[39] Illers KH, Breuer H. J Colloid Sci 1963;18:1–31.
[40] Maxwell AS, Monnerie L, Ward IM. Polymer 1998;39:6851–9.
[41] Maxwell AS, Ward IM, Laupretre F, Monnerie L. Polymer 1998;39:6835–49.